

**INTERFACIAL REACTIONS AND ELECTROMIGRATION IN LEAD-FREE SOLDER JOINTS  
WITH COPPER AND Au-Ni SURFACE FINISHED COPPER SUBSTRATES**

**DUONG NGOC BINH**

**UNIVERSITI SAINS MALAYSIA**

**2009**

**INTERFACIAL REACTIONS AND ELECTROMIGRATION IN LEAD-FREE SOLDER JOINTS  
WITH COPPER AND Au-Ni SURFACE FINISHED COPPER SUBSTRATES**

**by**

**DUONG NGOC BINH**

**Thesis submitted in fulfillment of the**

**requirements for the degree of**

**Doctor of Philosophy**

**November 2009**

## **ACKNOWLEDGEMENTS**

I would like to express my sincere gratitude to my supervisor, Professor Dr. Radzali Othman. I also would like to thank Assoc. Prof. Dr. Luay Bakir Hussain, my late supervisor. Their understanding, encouraging and personal guidance have provided a good basis for the present work.

I wish to express my warm and sincere thanks to my co-supervisor, Professor Dr. Tadashi Ariga, who was constantly taking a good care of me especially for the year in Japan. I would also like to gratefully acknowledge Dr. Ahmad Badri Ismail, my other co-supervisor, for his constant supporting and guidance during my study.

I also warmly thank to Prof. Dr. Khairun Azizi Mohd Azili, Director – Engineering Campus, Universiti Sains Malaysia, Assoc. Prof. Dr. Nguyen Hong Hai, Deputy Dean - Faculty of Materials Science, Hanoi University of Technology and all the staffs and technicians of the school of Materials and Mineral Resources Engineering for their kindness and support.

Furthermore, I am deeply grateful to the financial support and caring from AUN/SEED-Net, JICA. I also wish to thank Mr. Yamada and Ms. Kalayaporn for their support and caring.

## TABLE OF CONTENTS

ACKNOWLEDGEMENTS.....	ii
TABLE OF CONTENTS.....	iii
LIST OF TABLES.....	vii
LIST OF FIGURES .....	viii
ABSTRAK.....	xii
ABSTRACT.....	xiii

### Chapter one: INTRODUCTION

1.1 General.....	1
1.2 Problem statement.....	3
1.3 Objectives of Study.....	7

### Chapter two: LITERATURE REVIEW

2.1 Solder and soldering.....	8
2.2 Solder in microelectronic.....	9
2.3 Lead-bearing solders.....	11
2.4 Lead-free solders.....	13
2.4.1 The tin (Sn) element.....	15
2.4.2 Tin-silver (Sn-Ag) solder alloys.....	16
2.4.3 Tin-bismuth (Sn-Bi) solder alloys.....	19
2.4.4 Tin-indium (Sn-In) solder alloys.....	21
2.4.5 Tin-zinc solder alloys.....	23
2.5 Properties of solder alloys.....	24
2.5.1 Melting temperature.....	24

2.5.2	Wetting characteristics.....	28
2.5.2.1	Surface tension.....	32
2.5.2.2	Contact angle .....	34
2.5.2.3	Wetting Force.....	38
2.6	Solder substrate interaction.....	41
2.6.1	Interfacial reaction between copper (Cu) and tin (Sn).....	42
2.6.2	Interfacial reaction between nickel (Ni) and tin (Sn).....	45
2.6.3	Interfacial reaction between gold (Au) and tin (Sn) .....	50
2.7	Electromigration.....	53

### Chapter three: EXPERIMENTAL

3.1	Raw materials.....	58
3.1.1	Solder Alloys .....	58
3.1.2	Substrates .....	59
3.1.3	Fluxes.....	60
3.2	Experiments .....	60
3.2.1	Wetting Balance test .....	60
3.2.2	Spreading test.....	62
3.2.3	Electromigration experiment .....	64
3.3	Specimen characterization .....	66
3.3.1	Solder spreading area measurement.....	66
3.3.2	Contact angle measurement .....	68
3.3.3	Intermetallic compound (IMC) thickness measurement.....	69
3.3.4	Sample preparation for microstructural analysis .....	69

## Chapter four: RESULTS AND DISCUSSION

4.1	Microstructure of solder alloys .....	71
4.2	Wetting Characteristics .....	74
4.2.1	Spreading .....	74
4.2.1.1	Spreading area of solder alloys .....	74
4.2.1.2	Contact angle of solder alloys.....	80
4.2.1.3	Intermetallic compound formation during spreading test.....	85
4.2.2	Wetting balance .....	98
4.2.2.1	Effect of temperature, flux and substrate on wetting time.....	100
4.2.2.2	Effect of temperature, flux and substrate on maximum wetting force .. .....	109
4.2.2.3	Microstructure of the IMC formed during wetting balance test .....	116
4.3	Electromigration effect in lead-free in solder joints .....	118
4.3.1	Intermetallic compounds formed at the solder-substrate interface .....	118
4.3.2	Intermetallic growth in lead-free solder joints subjected to electromigration .....	122
4.3.3	Microstructure of solder joint subjected to electromigration.....	138
4.3.4	The formation of IMC sub-layer.....	141

## Chapter five: CONCLUSION

5.1	Conclusions .....	144
5.2	Future works .....	145

## LIST OF TABLES

Table 2.1 Important properties of solder alloys .....	14
Table 2.2 Melting/liquidus temperatures of lead and lead-free solder alloys.....	26
Table 2.3 Measured values of surface tension .....	33
Table 2.4 Natural radius of curvature, R, of lead-free solder alloys.....	33
Table 2.5 Contact angle of lead-free solders .....	35
Table 2.6 Contact angle of solder alloys.....	37
Table 2.7 Wetting force of lead-free solders on Cu substrate.....	40
Table 2.8 Wetting force on Cu Substrate, at 62°C above melting point.....	41
Table 4.1 Calculated diffusion coefficient of solder alloys .....	137

## LIST OF FIGURES

Figure 2.1 Solder used to joint metallic parts together .....	8
Figure 2.2 Wire bonding and flip-chip technology.....	9
Figure 2.3 Solder joint in electronic assembly.....	10
Figure 2.4 Cross-section of a flip-chip connection.....	11
Figure 2.5 Tin-silver phase diagram .....	17
Figure 2.6 Microstructure of eutectic Sn-Ag/Cu solder joint .....	18
Figure 2.7 Tin-bismuth phase diagram .....	19
Figure 2.8 Microstructure of eutectic Bi-Sn solder alloy .....	20
Figure 2.9 In-Sn phase diagram.....	21
Figure 2.10 Microstructure of eutectic In-Sn solder joint.....	22
Figure 2.11 Tin-zinc phase diagram .....	23
Figure 2.12 Microstructure of Sn-9Zn/Cu solder joint .....	24
Figure 2.13 Diagram of a contact angle.....	29
Figure 2.14 Relation between contact angle and degree of wetting .....	29
Figure 2.15 Copper-tin phase diagram.....	43
Figure 2.16 Ni-Sn phase diagram .....	46
Figure 2.17 Au-Sn phase diagram .....	50



Figure 2.18 Micrograph from the tip of the Au wire used in the wetting balance experiments .....	51
Figure 3.1 Solder alloys used in this study .....	58
Figure 3.2 Substrates used in this study.....	59
Figure 3.3 Diagram of substrate Type A cross-section.....	59
Figure 3.4 Fluxes used in this study.....	60
Figure 3.5 Schematic diagram of wetting balance test .....	61
Figure 3.6 Wetting balance test on a SAT-5100 Solder Checker .....	62
Figure 3.7 (a) Spreading test on a SAT-5100 Solder Checker, (b) Specimen before testing and (c) Specimen after testing .....	63
Figure 3.8 Soldering process.....	65
Figure 3.9 Diagram of electromigration test.....	65
Figure 3.10 (a) Electromigration specimen and (b) cross-section of the solder joint	66
Figure 3.11 Measuring spreading area using ImageJ software.....	67
Figure 3.12 Schematic diagram of contact angle measurement .....	68
Figure 3.13 SEM image of solder-substrate interface .....	69
Figure 4.1 Microstructure of (a) Sn-9Zn, (b) Sn-8Zn-3Bi and (c) Sn-3Ag-0.5Cu solder alloys at low magnification (left) and high magnification (right) .....	72
Figure 4.2 Spreading of (a) Sn-3Ag-0.5Cu, (b) Sn-9Zn and (c) Sn-8Zn-3Bi solder alloys on Au-Ni surface finished copper substrate.....	75
Figure 4.3 Intermediate zone in spreading specimen of Sn-8Zn-3Bi .....	76

Figure 4.4 Spreading areas of lead-free solders on several Au-Ni surface finished substrates .....	78
Figure 4.5 Contact angles of different lead-free solder alloys on different thickness of Au-Ni surface finished copper substrate. ....	81
Figure 4.6 SEM images of intermetallic layer formed between Sn-9Zn and Au0.5 substrate.....	85
Figure 4.7 EDX analysis result of IMC formed between Sn-9Zn and Au0.5 substrate .....	86
Figure 4.8 Au-Zn phase diagram. ....	87
Figure 4.9 SEM images of Sn-9Zn and Au-Ni surface finished copper substrate interface: (a) Au0.5, (b) Au0.3 and (c) Au0.1 .....	88
Figure 4.10 IMC formed between Sn-9Zn and Au0.3 substrate.....	89
Figure 4.11 IMC formed between Sn-9Zn and Au0.1 substrate.....	90
Figure 4.12 IMC formed between Sn-8Zn-3Bi and Au0.5 substrate.....	91
Figure 4.13 EDX analysis result of IMC at Sn-8Zn-3Bi and Au0.5 substrate interface .....	92
Figure 4.14 IMC formed between Sn-8Zn-3Bi and Au0.3 substrate.....	93
Figure 4.15 IMC formed between Sn-8Zn-3Bi and Au0.1 substrate.....	93
Figure 4.16 IMC formed between Sn-3Ag-0.5Cu and Au-Ni surface finished substrate .....	94
Figure 4.17 EDX analysis result of IMC in Sn-3Ag-0.5Cu solder with Au0.5 substrate .....	95
Figure 4.18 EDX analysis result of IMC at Sn-3Ag-0.5Cu and Au0.5 substrate interface .....	96

Figure 4.19 Typical wetting force curve obtained from the wetting balance test.....	98
Figure 4.20 Diagram of substrate dipped into molten solder.....	99
Figure 4.21 Wetting times of Sn-9Zn on Au-Ni surface finished copper substrate using (a) MHS flux and (b) RMA flux.....	101
Figure 4.22 Wetting time of Sn-8Zn-3Bi on Au-Ni surface finished copper substrate .....	104
Figure 4.23 Wetting force curves of Sn-8Zn-3Bi on Au0.5 substrate and RMA flux .....	105
Figure 4.24 Wetting time of Sn-3Ag-0.5Cu on Au-Ni surface finished copper substrate.....	106
Figure 4.25 Wetting time of Sn-8Zn-3Bi on Au0.3 substrate.....	108
Figure 4.26 Wetting force of Sn-9Zn on Au-Ni surface finished substrate with (a) MHS flux and (b) RMA flux.....	111
Figure 4.27 Wetting force of Sn-8Zn-3Bi on Au-Ni surface finished substrate with (a) MHS flux and (b) RMA flux.....	113
Figure 4.28 Wetting force of Sn-3Ag-0.5Cu on Au-Ni surface finished substrate with (a) MHS flux and (b) RMA flux. ....	115
Figure 4.29 Solder substrate interface after wetting balance test (a) Sn-3Ag-0.5Cu, (b) Sn-8Zn-3Bi and (c) Sn-9Zn.....	117
Figure 4.30 Movement of the solder and substrate in the (a) spreading test and (b) wetting balance test .....	118
Figure 4.31 SEM image of Sn-3Ag-0.5Cu/Cu interface after soldering .....	119
Figure 4.32 SEM image of Sn-9Zn/Cu interface after soldering.....	121
Figure 4.33 SEM image of Sn-8Zn-3Bi/Cu interface after soldering.....	121

Figure 4.34 Thickness of IMC layer in Sn-9Zn solder joint subjected to electromigration: (a) Anode, (b) Cathode .....	123
Figure 4.35 Thickness of IMC layer in Sn-8Zn-3Bi solder joint subjected to electromigration: (a) Anode, (b) Cathode .....	124
Figure 4.36 Thickness of IMC layer in Sn-3Ag-0.5Cu solder joint subjected to electromigration: (a) Anode, (b) Cathode .....	125
Figure 4.37 Thickness of IMC layer for all three solder joints subjected to electromigration at 300A/cm <sup>2</sup> .....	127
Figure 4.38 (a) Schematic diffusion couple A-B, (b) The composition profile of species A within the intermetallic layer, showing how the concentration gradient is reduced when greater composition steps are needed at the $\alpha/\beta$ and $\beta/\gamma$ interfaces to drive their migration.....	129
Figure 4.39 IMC thickness of all the solder alloys at 300A/cm <sup>2</sup> .....	133
Figure 4.40 Diagram of diffusion in a solder joint .....	134
Figure 4.41 Thickness of IMC subjected to square root of time .....	136
Figure 4.42 Microstructure of solder joint subjected to electromigration .....	138
Figure 4.43 SEM images of the Sn-9Zn/Cu interface.....	139
Figure 4.44 SEM image of the interface of Sn-3Ag-0.5Cu/Cu solder joint .....	140
Figure 4.45 Sn-3Ag-0.5Cu/Cu interface after 120h electromigration at 500A/cm <sup>2</sup>	141
Figure 4.46 Sn-9Zn/Cu interface after 120h electromigration at 500A/cm <sup>2</sup> .....	143

**TINDAKBALAS ANTARAMUKA DAN MIGRASI-ELEKTRO DALAM SAMBUNGAN  
PATERI BEBAS PLUMBUM KE ATAS KEMASAN PUMUKAAN KUPRUM DAN Au-Ni**

**ABSTRAK**

Pencirian aloi pateri tanpa plumbum (Sn-9Zn, Sn-8Zn-3Bi dan Sn-3Ag-0.5Cu) ke atas substrat kumprum tanpa salutan dan yang disalut dengan Au-Ni telah dilakukan. Keputusan menunjukkan kebolehasahan bagi ketiga-tiga aloi pateri ke atas substrat kuprum adalah baik pada suhu yang telah ditetapkan. Ukuran sudut sentuh dan daya basahan menunjukkan pembasahan yang baik telah tercapai. Analisis mikrostruktur antaramuka bagi aloi pateri dan substrat kuprum bersalut Au-Ni pula menunjukkan lapisan Au pada substrat telah terlarut sepenuhnya ke dalam aloi pateri selepas 20 saat. Lapisan antaralogam Au-Zn yang telah terbentuk adalah  $Au_5Zn_3$  pada Sn-9Zn dan  $AuZn_3$  pada Sn-8Zn-3Bi. Antaralogam  $AuSn_4$  pula telah ditemui di dalam aloi pateri Sn-3Ag-0.5Cu. Lapisan antaralogam  $(Ni,Cu)_6Sn_5$  yuga telah terbentuk antara antaralogam aloi pateri dan substrat. Migrasi-elektro menyebabkan penebalan lapisan antaralogam  $Cu_5Zn_8$  pada sambungan antaramuka di dalam Sn-9Zn serta sambungan Sn-8Zn-3Bi, dan  $Cu_6Sn_5$  pada sambungan Sn-3Ag-0.5Cu. Proses penebalan berlaku pada kadar yang berbeza. Penebalan IMC diperhatikan lebih pantas pada anod spesimen berbanding pada katod. Selain itu, lapisan  $Cu_5Zn_8$  yaus turut terbentuk pada sambungan Sn-9Zn dan Sn-8Zn-3Bi membentuk dengan lebih cepat berbanding  $Cu_6Sn_5$  pada sambungan Sn-3Ag-0.5Cu. Arus elektrik juga memberi kesan kepada ke atas  $Cu_6Sn_5$  di dalam Sn-3Ag-0.5Cu dengan  $Cu_6Sn_5$  bak jejarum terbentuk sepanjang arah arus.

**INTERFACIAL REACTIONS AND ELECTROMIGRATION IN LEAD-FREE SOLDER JOINTS WITH  
COPPER AND Au-Ni SURFACE FINISHED COPPER SUBSTRATES**

**ABSTRACT**

Properties of lead free solder alloys (Sn-9Zn, Sn-8Zn-3Bi and Sn-3Ag-0.5Cu) on Au-Ni surface finished copper and copper substrates were investigated. Results obtained showed good wetting of all three solder alloys on Au-Ni surface finished substrate at appropriate temperatures. Contact angle measurement and wetting force results reaffirmed that good wetting of solder alloys on substrate was achieved. Microstructural analysis of the interface between solder alloys and Au-Ni surface finished copper substrate revealed that the Au layer on the substrate had dissolved completely into solder alloys after 20 seconds. A layer of Au-Zn intermetallic compound (IMC) was formed at the solder substrate interface, i.e.  $Au_5Zn_3$  in Sn-9Zn and  $AuZn_3$  in Sn-8Zn-3Bi. With Sn-3Ag-0.5Cu,  $AuSn_4$  IMCs were found distributed in the solder alloy and a layer of  $(Ni,Cu)_6Sn_5$  IMC was formed at the solder-substrate interface. Electromigration has thickened the IMC layer at the interface of solder joint, which is  $Cu_5Zn_8$  IMC in Sn-9Zn and Sn-8Zn-3Bi joints whilst it is  $Cu_6Sn_5$  in the Sn-3Ag-0.5Cu joint. The thickening process occurred at different rates, faster IMC thickening was observed on the anode of a specimen than on the cathode. Also, the  $Cu_5Zn_8$  layer which is formed in the Sn-9Zn and Sn-8Zn-3Bi solder joints were found to grow faster than the  $Cu_6Sn_5$  layer in the Sn-3Ag-0.5Cu joint. Electric current was found to have an effect on the growth of  $Cu_6Sn_5$  in Sn-3Ag-0.5Cu, with elongated  $Cu_6Sn_5$  phase being formed along with the current direction.

# CHAPTER ONE

## INTRODUCTION

### 1.1 General

Rapid advances in microelectronic design and technology in recent decades have made modern day electrical and electronic equipment (EEE) obsolete within a very short period after their purchase resulting in mountains of electronic waste (e-waste) to be dealt with in many countries around the world. United Nations estimate that collectively the world generates 20 to 50 million tons of e-waste every year (Schwarzer *et al.*, 2005). The average lifespan of a new model computer has decreased from 4.5 years in 1992 to an estimated 2 years in 2005 and is further decreasing (Widmer *et al.*, 2005). E-waste is also one of the fastest growing waste streams around the world today growing at a rate of 3 to 5% per annum and around three times faster than normal municipal solid waste (Schwarzer *et al.*, 2005). Studies have revealed that around 500 million computers will become obsolete in the United States alone between 1997 and 2007 (Yu *et al.*, 2006) and every year over 130 million mobile phones in the United States and over 105 million mobile phones in Europe reach their end-of-life stage and are thrown away (Canning, 2006).

E-waste is a health and environmental concern due to the toxicity of some of the materials present in the waste stream. These include metals such as lead, mercury, hexavalent chromium and cadmium, and chemicals such as polychlorinated biphenyls. Among those metals, lead is of major concern due to the extensive use of

lead-bearing solders, especially the eutectic tin-lead (Sn-37Pb) or near-eutectic Sn-40Pb alloys, in the assembly of modern electronic circuits.

Lead has the ability to leach from landfills and contaminate the human food chain causing serious health hazards. Human toxicity of lead could result in cancer and could also adversely affect the liver and thyroid functions and the resistance to disease. Lead can affect almost every organ in the body including the nervous system, kidneys, and reproductive system. The main effect of lead toxicity is on the central nervous system of the humans. High exposure of lead could also severely damage the brain and kidneys of humans and could lead to miscarriage in pregnant women. High levels of lead could also affect the brain development of children and organs responsible for sperm production in men. Ecological toxicity of lead could occur as a result of direct exposure of algae, invertebrates, and fish to lead. Fish exposed to high levels of lead could exhibit effects such as growth inhibition, mortality, reproductive problems, and paralysis. Furthermore, at elevated levels of lead, plants could experience reduced growth, photosynthesis, and water absorption. Birds and mammals could also suffer from lead poisoning resulting in damage to nervous system, kidneys, and liver (ATSDR, 2005).

Due to the toxicity of lead, legislations have been imposed to limit the usage of lead-bearing solders. In Europe, The Directive on the Restriction of the Use of Certain Hazardous Substances in Electrical and Electronic Equipment (commonly referred to as the Restriction of Hazardous Substances Directive or RoHS) took effect on 1 July 2006. The RoHS restricts the use of six substances including lead (Pb), mercury (Hg) and cadmium (Cd) (European Union, 2003).



In Japan, Japanese law also mandates the take-back of various household electrical appliances to reuse and recycle materials and substances in those electrical appliances. Japanese companies have generally adopted the “green electronics” movement for environmental consciousness and market differentiation, and the electronics industry has widely transitioned to lead-free products (Pecht, 2004).

In the United States, legislation to limit the use of lead has been introduced in both the Senate and the House of Representatives (Abtew and Selvaduray, 2000). New measures are being considered in several states that would require recycling of consumer electronics. The Environmental Protection Agency has recently required industry to report discharges of lead into the environment at a much lower level, 10 pounds in every 10,000 pounds used (Zeng *et al.*, 2002)

## **1.2 Problem statement**

Due to the restriction of lead usage, finding alloys that can replace lead-bearing solders in electrical and electronic equipment (EEE) is critical in the electronic industry. There are numbers of lead-free solders that have been developed in order to replace the traditional Sn-Pb solders. However, finding a suitable substitute which satisfies all the requirements is not a simple matter. Although several lead-free solders are commercially available, none of them meets all the requirements which include low melting temperature, wettability, mechanical integrity, good manufacturability and affordable cost. Therefore, research on lead-free solders remains as an important issue in the electronic industry.

Among all the lead-free solders that have been developed, tin-silver-copper (Sn-Ag-Cu) alloys have been regarded as one of the most promising candidates to replace Sn-Pb solder due to their superior mechanical properties of strength, creep, and fatigue resistance (Zeng *et al.* 2002; Laurila *et al.*, 2005). However, a major drawback of the Sn-Ag-Cu solder is that their melting temperatures are nearly 30°C higher than that of the conventional Sn-Pb eutectic solder (melting temperature of Sn-Pb eutectic solder is 183°C), or in the case of Sn-3Ag-0.5Cu alloy in which the liquidus temperature is 220°C, the difference being almost 40°C.

Other candidates to substitute Sn-Pb is the eutectic and near eutectic tin-zinc (Sn-Zn) which have melting temperatures lower than that of Sn-Ag-Cu. The melting temperature of eutectic Sn-Zn is 198°C. The Sn-Zn alloys possess the advantages of high strength, good creep resistance, and high thermal fatigue resistance (Chiu *et al.*, 2002). However, the Sn-Zn system solders show poor wetting during soldering to electrodes (Iwanishi *et al.*, 2003), poor oxidation resistance in reflow soldering and may cause soldering failures, such as poor wetting and non-wetting (Shohji *et al.*, 2004). The addition of bismuth (Bi) into Sn-Zn alloys increases wettability, lowers the solidus temperature and improves corrosion resistance (McCormack *et al.*, 1994). Thus, the Sn-Zn-Bi alloys are promising lead-free solder candidates with melting temperature closer to that of eutectic Sn-Pb alloy.

While looking for an alloy to replace the traditional Sn-Pb eutectic, intermetallic formation between solder alloy and base metal is also an important issue. It is common knowledge that too much intermetallic within a joint can cause

embrittlement. For example, it is noted that in excess of 4wt% of gold in tin-lead joints can cause embrittlement (Ainsworth, 1971; Denman, 1996). This corresponds to the point at which the  $\text{AuSn}_4$  crystals start to be formed as massive primary species, rather than as part of a fine eutectic structure (which is what happens at lower gold contents).

Small amounts of intermetallic compounds, however, can produce distinct improvements in mechanical and thermal properties. For example, the most widely used lead-free solder alloys are based on the tin-silver and tin-copper eutectic systems. These alloys consist of a mixture of tin solid solutions and the intermetallic compounds  $\text{Ag}_3\text{Sn}$  and  $\text{Cu}_6\text{Sn}_5$ . Addition of silver and copper at levels up to the respective binary eutectic compositions (i.e. Sn-0.7Cu and Sn-3.5Ag) have the beneficial effects of reducing the liquidus temperature of the alloys, to 227°C and 221°C, respectively (melting temperature of Sn is 232°C). These additions also improve hardness and resistance to fatigue, which is arguably the most common cause of joint failures. Hence, the total quantity of intermetallic present is not the only factor, the morphology and distributions of the compounds are also very important.

Legislation is driving major changes in the manufacture of electrical and electronics equipment. The most significant change is the elimination of lead from solder joints. With the requirement to install lead-free solder processes, companies have a choice of alloys. One consumer electronics company used a four-stage selection process to make this decision. This process included (Boone *et al.*, 2005):

- Determining the criteria that need to be considered when making the selection: process yield, process maintenance, component and board compatibility, in-service reliability and total cost of ownership.
- Initial screening of available alloys and the generation of a short list.
- Process yield experimentation - design of experiment setup, optimized process settings.
- Reliability testing - final stage of the alloy selection process, involving thermal cycle and extensive joint examination.

As the selection process does not have any detail requirement on the alloys property (only reliability test included), some solder alloys are being used without fundamental knowledge of the alloys. As a consequence, some lead free solders are commercially available but have not yet been fully characterized. Therefore, further study on such alloys remains an important issue. The Sn-3Ag-0.5Cu, Sn-9Zn and Sn-8Zn-3Bi are examples of alloys being made commercially available without detail knowledge on their properties. While those alloys and Au-Ni surface finished copper substrate are commercially available, information on reactions between solder and substrate, electromigration in the solder joint are insufficient. Thus, further investigations on the properties of those alloys are required and this becomes the thrust in this research work.

### 1.3 Objectives of Study

In this work, properties of tin-silver-copper (Sn-3Ag-0.5Cu), tin-zinc (Sn-9Zn) and tin-zinc-bismuth (Sn-8Zn-3Bi) solder alloys were investigated.

The main objectives of this work include:

1. A study on the solder-substrate interactions.
  - Wetting behavior of lead free solder alloys on Au-Ni surface finished copper substrate
  - Intermetallic compound formation at the solder-substrate interface
2. A study on electromigration effect on the formation and growth of intermetallic compounds (IMC) at the solder-substrate interface in solder joints

## CHAPTER TWO

### LITERATURE REVIEW

#### 2.1 Solder and soldering

Soldering is a metallurgical joining method that uses a filler metal, the solder, with a melting point below 425°C (Manko, 1979), to join metallic parts together (Figure 2.1).

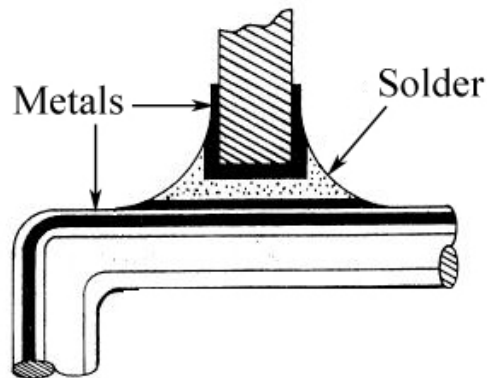


Figure 2.1 Solder used to joint metallic parts together (Manko, 1979)

The practice of soldering has been in existence for some time. While there is evidence to suggest that it was used even earlier, many different soldering techniques were widely used throughout the Greek and Roman Empires, as well as in Viking dominated Scandinavia. Archeologists have found jewelry, weapons, tools and cutlery that have been very skillfully soldered (Frear, 2002). Throughout the years solder has been used in various applications; however it was the invention of electronic devices in the latter part of the 20th century that led to rapid advances in soldering technologies.

## 2.2 Solder in microelectronic

In the immense electronic materials world, solder plays a crucial role in the assembly and interconnection of silicon die (or chip). As a joining material, the solder provides electrical, thermal and mechanical connection in electronic assemblies. The performance and quality of solder are crucial to the integrity of a solder joint which in turn is vital to the overall functioning of the assembly.

As a die bonding material, the solder provides the electrical and mechanical connection between the silicon die and the bonding pad. It also serves as a path for dissipation of the heat generated by the semiconductor. Bonding of the die to a substrate and its encapsulation is referred to as Level 1 packaging. While the predominant method of providing electrical connection to the silicon chip is through wire bonding (Figure 2.2), the use of solder bumps on the surface of the Si die, instead of wire bonding, has been gaining acceptance due to the higher number of input/output terminals that can be attached to a given area (Zeng *et al.*, 2002). The flip chip configuration, which is also shown in Figure 2.2, is an approach to increase the number of input/output terminals.

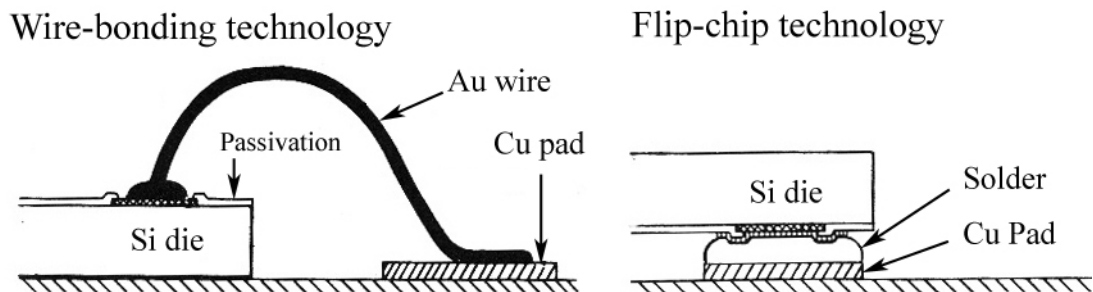


Figure 2.2 Wire bonding and flip-chip technology (Abteew and Selvaduray, 2000)

The next level of assembly and interconnect, referred to frequently as Level 2 packaging, is where the component (encapsulated silicon die) is mounted on a printed wiring board (PWB). Solder is the primary means of interconnect in Level 2 packaging. Practically all microelectronic devices (also known as packages) are mounted on PWBs using solders (Abtew and Selvaduray, 2000). There are two primary means of attaching electronic components to PWBs - pin-through-hole (PTH) or surface mount technology (SMT), illustrated in Figure 2.3.

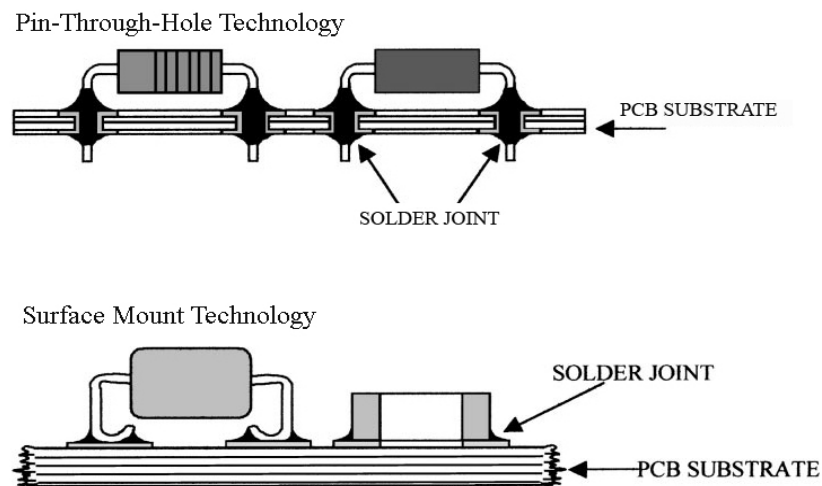


Figure 2.3 Solder joint in electronic assembly (Abtew and Selvaduray, 2000)

Solder usage had been restricted primarily to the board level assembly process, i.e. Level 2 packaging, with very little being used in Level 1 packaging. However, with the advent of area array packaging concepts (flip chip and ball grid arrays), usage of solders in Level 1 packaging is increasing.

In the “flip chip” approach the silicon die has an array of solder balls placed on its surface, as shown in Figure 2.4. The solder balls are attached to the substrate,



and the entire assembly is processed through a reflow oven. The solder ball melts and forms solder joints between the silicon die and substrate.

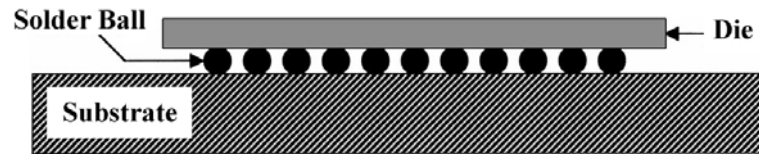


Figure 2.4 Cross-section of a flip-chip connection (Abtew and Selvaduray, 2000)

### 2.3 Lead-bearing solders

Lead-bearing solder, especially tin-lead solders and the alloys developed based on tin-lead have long provided and continue to provide many benefits, such as ease of handling, low melting temperatures, good workability, ductility, and excellent wetting on copper and its alloys. As one of the primary constituents in solder alloys, lead provides many technical advantages and these include the following:

- Pb provides the ductility in Sn-Pb solders (Zeng *et al.*, 2002).
- Eutectic Sn-Pb has a low melting temperature of 183°C so the reflow temperature is low - typically around 200°C (Zeng *et al.*, 2002). Thus, degradation in polymeric material used in assembly can be avoided.
- Pb reduces the surface tension of pure tin, which is 550 mN/m at 232°C, and the lower surface tension of Sn-37Pb solder (470 mN/m at 280°C) facilitates wetting (Vianco, 1993). Wetting angle of molten

eutectic Sn-Pb on Cu is 11° and that of pure tin is 35° (Kim *et al.*, 1995).

- As an impurity in tin, even at levels as low as 0.1 wt.%, Pb prevents the transformation of white or beta ( $\beta$ ) tin to gray or alpha ( $\alpha$ ) tin upon cooling past 13°C. The transformation, if it occurs, results in a 26% increase in volume and causes loss of structural integrity to the tin (Reed-Hill, 1994).
- Pb serves as a solvent metal, enabling the other joint constituents such as Sn and Cu to form intermetallic bonds rapidly by diffusing in the liquid state (Abtew and Selvaduray, 2000).

These factors, combined with Pb being readily available and a low cost metal, make it an ideal alloying element with tin. The board level soldering system that is mainly based on eutectic and near eutectic Sn-Pb solders has been well developed and refined with many years of experience. A relatively well-established knowledge base about the physical metallurgy, mechanical properties, flux chemistries, manufacturing processes and reliability of eutectic Sn-Pb solders exists. Board level assembly and soldering equipment are almost exclusively engineered with Sn-Pb solder in mind. A good understanding of the behavior of Sn-Pb solders has enabled current board level technology to assemble and create small geometry solder joints, approaching 75  $\mu$ m in size, in high volume, and at competitive cost (Abtew and Selvaduray, 2000).

## **2.4 Lead-free solders**

There are strict performance requirements for solder alloys used in microelectronics. In general, the solder alloy must meet the expected levels of electrical and mechanical performance, and must also have the desired melting temperature. It must adequately wet common print circuit board (PCB) materials, form inspectable solder joints, allow high volume soldering and rework of defective joints, provide reliable solder joints under service conditions and must not significantly increase assembly cost.

When trying to identify an alternative to the current Pb-Sn solders that are widely used, it is important to ensure that the properties of the replacement solder are comparable to or superior than Pb-Sn solders. The major performance characteristics of solders that are of importance for second level packaging applications are manufacturability, reliability and environmental suitability. Manufacturability describes how well a Pb-free solder fits into current second level packaging practices without requiring significant changes. Manufacturability involves most of the physical properties of a solder alloy relevant to soldering such as melting temperature, solderability, viscosity, density, thermal and electrical properties, corrosion and oxidation behavior, surface tension, reworkability and cost. Reliability of a solder alloy for the first and second level packaging is mainly dependent on the coefficient of thermal expansion, elastic modulus, yield strength, shear strength, fatigue and creep behavior of the alloy. A Pb-free alloy also needs to be environmentally friendly. The properties of solders that are of importance from a manufacturing and also long-term reliability standpoint are summarized in Table 2.1.

Table 2.1 Important properties of solder alloys (Abteu and Selvaduray, 2000)

Properties relevant to manufacturing	Properties relevant to reliability and performance
Melting/liquidus temperature	Electrical conductivity
Wettability (of copper)	Thermal conductivity
Cost	Coefficient of thermal expansion
Environmental friendliness	Shear properties
Availability and number of suppliers	Tensile properties
Manufacturability using current processes	Creep resistance
Ability to be made into balls	Fatigue properties
Copper pick-up rate	Corrosion and oxidation resistance
Recyclability	Intermetallic compound formation
Ability to be made into paste	

Ever since the commencement of the research and development of lead-free solder, a relatively large number of lead-free solder alloys have been proposed. Abteu and Sevaduray (2000) have identified as much as 69 lead-free solder alloys from the literature. The solder alloys are binary, ternary and even quaternary alloys. The element tin makes an appearance in almost all alloys with the composition varying from 17 wt. % (Bi-26In-17Sn) to 99.25 wt. % (Sn-0.75Cu).

Surprisingly, amongst all 69 lead-free alloys listed, there are a number of alloys that contain antimony (Sb) with Sb composition varying from 0.5 wt. % (Sn-2.5Ag-0.8Cu-0.5Sb, Sn-10In-1Ag-0.5Sb) to 10 wt. % (Sn-25Ag-10Sb). The element antimony (Sb) is of certain toxicity and therefore, an antimony-bearing solder should not be considered as an alternative for lead-bearing solder. It is believed that those alloys were proposed in order to meet the requirements of legislations that restrict the use of lead at that time. In recent studies, there is little continuing research on Sb-bearing solders.

As the rapid development of the electronic industry takes place, the number of lead-free solders being introduced has significantly increased. The Sn-8Zn-3Bi

which is not included in Abtew's list is now commercially available. Nevertheless, other new lead-free solder alloys developed are still based on tin and tin alloys. Since the properties of the binary Pb-free solders cannot fully meet the requirements for applications in electronic packaging, additional alloying elements were added to improve the performance of these alloys. Thus, ternary and even quaternary Pb-free solders have been developed. These solder alloys are of four common systems: tin-silver (Sn-Ag), tin-bismuth (Sn-Bi), tin-indium (Sn-In) and tin-zinc (Sn-Zn) with other alloying element such as Cu, Mg or in many cases, rare earth (RE) elements (Wu *et al.*, 2004).

#### **2.4.1 The tin (Sn) element**

The ability of tin to wet and spread on a wide range of substrates, using mild fluxes, has caused it to become the principal component of most solder alloys used for electronic applications. Elemental tin has a melting temperature of 231°C. Tin exists in two different forms with two different crystal structures in the solid state. White or  $\beta$ -tin has a body-centered tetragonal crystal structure and is stable at room temperature. Gray tin or  $\alpha$ -tin, which has a diamond cubic crystal structure, is thermodynamically stable below 13°C. The transformation of  $\beta$ -tin to  $\alpha$ -tin, also referred to as *tin pest*, takes place when the temperature falls below 13°C, and results in a large increase in volume, which can induce cracking in the tin structure. Due to its body centered tetragonal crystal structure that is anisotropic, the thermal expansion of tin is also anisotropic. Therefore, when tin is exposed to repeated thermal cycling, plastic deformation and eventual cracking at grain boundaries can occur. This effect has been observed in thermal cycling over a range as small as 30-

75°C. Thus, thermal fatigue can be induced in tin or tin-rich phases of solder alloys even when no external mechanical strain is imposed.

The addition of alloying agents has been reported to be effective in suppressing this phase transformation, thus ameliorating the problems associated with tin pest. According to Lewis (1961), the addition of greater than 0.5 wt.% Sb, 0.1 wt.% Bi, or over 5 wt.% Pb is effective in eliminating tin pest. However, the mechanisms via which these alloying agents contribute towards elimination of tin pest are not clear at this time. Taking the example of the Sn-Pb system, the solid solubility of Pb in Sn at 13°C is less than 0.3 wt.%. A Sn - 5 wt.% Pb alloy will be a two-phase alloy consisting of the Sn-rich and the Pb-rich phases. It is not clear if the Pb addition actually suppresses the  $\beta \rightarrow \alpha$  transformation in the Sn-rich phase, or if the Pb-rich phase 'absorbs' the volume expansion by plastically deforming, with the net result of an absence of the manifestation of tin pest on the macroscopic structure (Abtew and Selvaduray, 2000).

#### **2.4.2 Tin-silver (Sn-Ag) solder alloys**

The eutectic composition for the tin-silver (Sn-Ag) binary system occurs at Sn-3.5Ag and the eutectic temperature is 221°C. Binary phase diagram of Sn-Ag system is shown in Figure 2.5 (NIST, 2008).

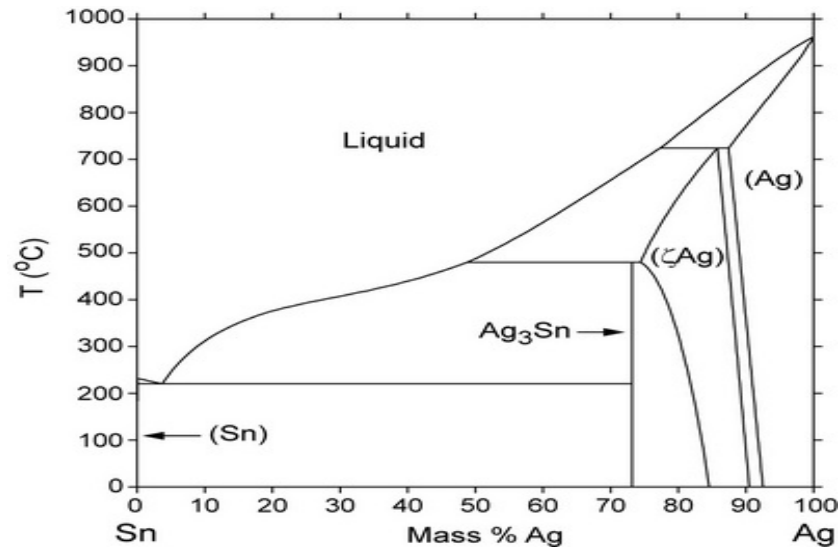


Figure 2.5 Tin-silver phase diagram (NIST, 2008)

Microstructure of eutectic Sn-Ag consists of Sn and the intermetallic  $Ag_3Sn$  in the form of thin platelets, as shown in Figure 2.6 (McCormack *et al.*, 1993; Yang and Messler, 1994). McCormack *et al.* described the solidified microstructure of the binary eutectic Sn-3.5%Ag as consisting of a  $\beta$ -Sn phase with dendritic globules and inter-dendritic regions with a eutectic dispersion of  $Ag_3Sn$  precipitates within a  $\beta$ -Sn matrix. Addition of 1% Zn has been shown to improve the solidification microstructure of this alloy by eliminating the large  $\beta$ -Sn dendritic globules and introducing a finer and a more uniform two-phase distribution throughout the alloy (McCormack *et al.*, 1995). The addition of Zn suppresses the formation of  $\beta$ -Sn dendrites and results in a uniform dispersion of  $Ag_3Sn$ . Similar to the Sn-0.07Cu alloy, this solder may be prone to whisker growth due to its high tin composition. However, there is no information available in the literature with regard to whisker growth in Sn-Ag (Abteu and Selvaduray, 2000).

Prabhu *et al.* (2004) reported that the evolution of the microstructure of a eutectic Sn-Ag alloy solidifying against a metallic substrate is highly sensitive to the surface texture of the substrate and the application of a flux coating on the substrate surface. The use of flux and increased roughness of the substrate seem to increase the cooling rate of the solidifying solder alloy. A transition from lamellar to a fine fibrous eutectic microstructure is observed as the surface condition of the substrate is altered from a smooth to a rough texture with a flux applied on its surface. This transition in the microstructure is found to be accompanied by an improvement in the quality of the joint at the solder/substrate interface.

Figure 2.6 shows the microstructure of a eutectic Sn-Ag/Cu solder joint made by reflow (Yang and Messler, 1994). The rod-like  $\text{Ag}_3\text{Sn}$  ( $\epsilon$ -phase) appears in a matrix of nearly pure Sn. The  $\epsilon$ -phase rods are perpendicular to the joint interface, reflecting the solidification direction of the solder. Cu-Sn intermetallic layers identified as  $\text{Cu}_6\text{Sn}_5$  phase were found at solder-copper interfaces.

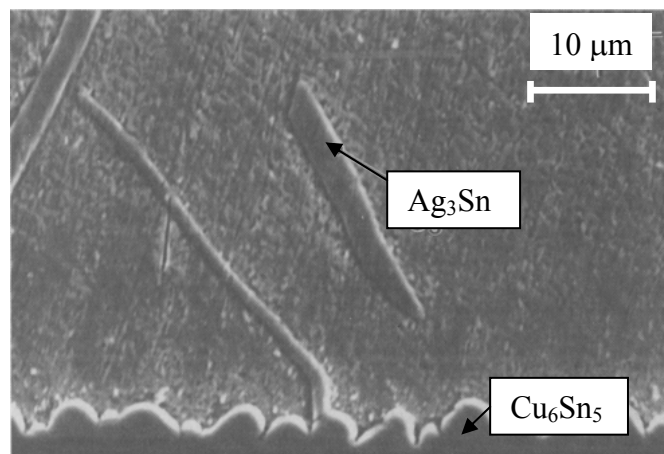


Figure 2.6 Microstructure of eutectic Sn-Ag/Cu solder joint (Yang and Messler, 1994)



### 2.4.3 Tin-bismuth (Sn-Bi) solder alloys

The tin-bismuth (Sn-Bi) system has a eutectic composition of 42Sn-58Bi and a relatively low eutectic temperature of 139°C, Figure 2.7 (NIST, 2008).

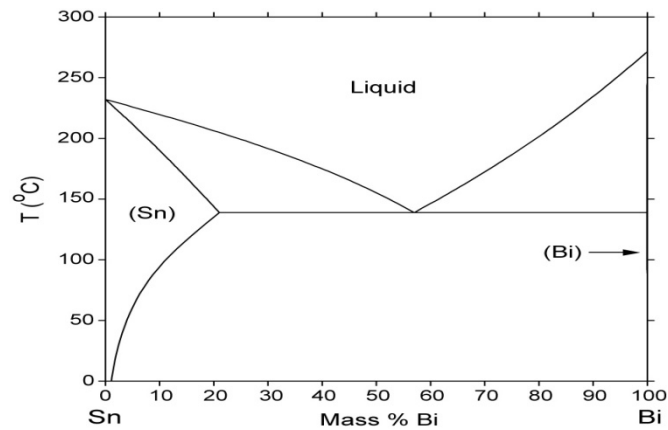


Figure 2.7 Tin-bismuth phase diagram (NIST, 2008)

The room temperature equilibrium phases are Bi and Sn with about 4 wt.% Bi in solid solution (Morris *et al.*, 1993). Since tin has a very low solubility in Bi at the eutectic solidification temperature of 130°C, the Bi phase is essentially pure Bi. However, the maximum solubility of Bi in Sn is about 21 wt.% (Kabassis *et al.*, 1986). As the alloy cools, Bi precipitates in the Sn phase. At moderate cooling rates, the eutectic Sn-Bi microstructure is lamellar, with degenerate material at the boundaries of the eutectic grains. This microstructure is similar to the one theoretically predicted by Croker *et al.* (1973) for relatively slow cooling rates.

Goldstein and Morris (1994) reported that eutectic Bi-Sn has a complex regular microstructure with complicated patterns. The microstructure consists of cells, with similar lamellar orientation within each cell. The cells appear either

triangular or rectangular in cross section. Occasionally isolated islands of Sn dendrites or faceted Bi particles are observed. The decrease in solid solubility of Bi in Sn as the alloy is cooled causes Bi precipitates to form within the Sn-rich regions of the eutectic. This precipitation can be seen within the Sn dendrites in Figure 2.8.

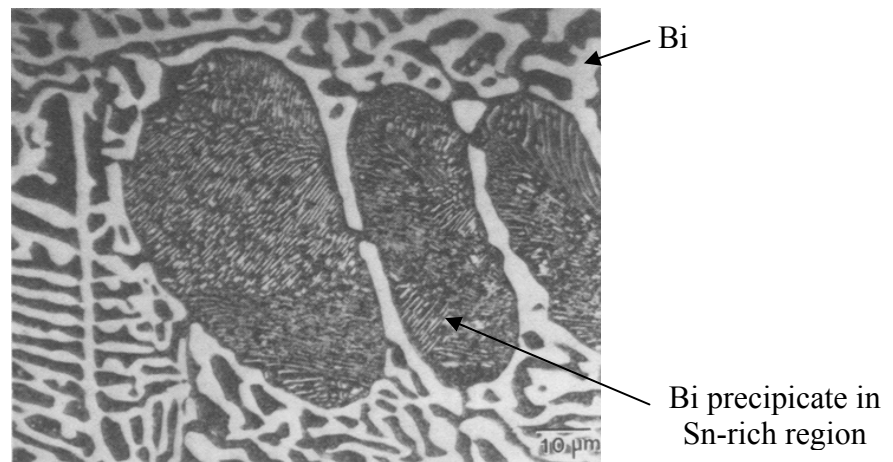


Figure 2.8 Microstructure of eutectic Bi-Sn solder alloy (Goldstein and Morris, 1994)

Wild (1971) observed cracks on slowly cooled eutectic Sn-Bi solder joints. Slow cooling resulted in the formation of large grains. Tin precipitates from the solder matrix along the boundaries of these large grains through which cracking occurs. Cracking was not observed during rapid cooling. Cooling rates, however, were not specified in the literature. It has also been reported by Glazer (1995) that recrystallization of the alloy produced an expansion of up to 0.0007 in./in. The expansion results in embrittlement, which may be due to strain hardening caused by deformation that occurs to accommodate the expansion (Wild, 1971).

#### 2.4.4 Tin-indium (Sn-In) solder alloys

The indium-based solder with the composition of In-48Sn is the one that is commonly used for surface mount technology (SMT) applications due to their substantially low melting temperature. The eutectic composition is In-48Sn, and the eutectic temperature is 117°C. Binary phase diagram of Sn-In system is shown in Figure 2.9 (Okamoto, 2006A). The two phases that form are intermetallic phases - an In-rich, pseudo-body-centered tetragonal phase,  $\beta$ , which has 44.8 wt.% Sn, and a hexagonal Sn-rich phase,  $\gamma$ , with 77.6 wt.% Sn (Glazer, 1995). Mei and Morris (1992) described the microstructure of In-48Sn solder on a Cu substrate as having lamellar features. The Sn-rich phase is composed of equiaxed grains. The In-rich phase contains Sn precipitates. A similar structure with less irregularity was observed by Freer and Morris on a Ni substrate (Freer *et al.*, 1992), and significant microstructural coarsening was observed by Seyyedi (1993), after prolonged aging of the solder joints made on a Cu substrate.

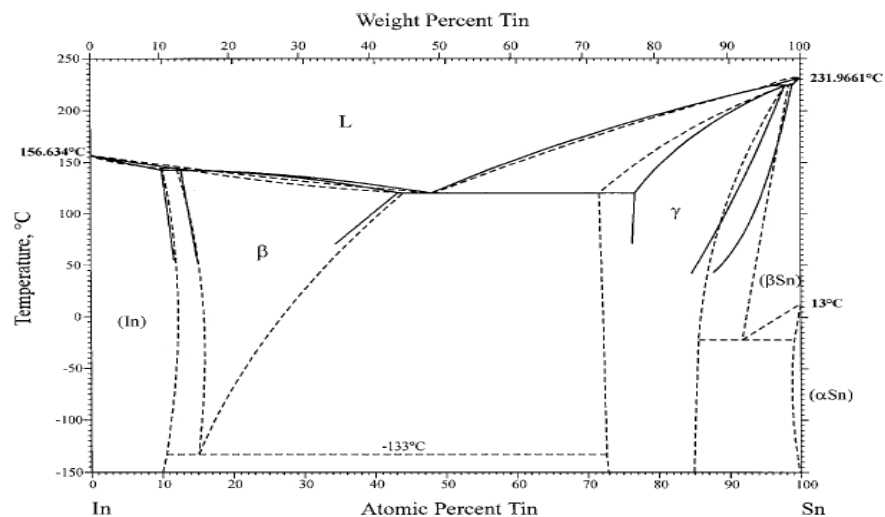


Figure 2.9 In-Sn phase diagram (Okamoto, 2006A)

Goldstein and Morris (1994) described the microstructure of eutectic In-Sn as an irregular microstructure. The microstructure consists of many dendrites of the  $\gamma$  Sn-rich phase on In-rich matrix (Figure 2.10).

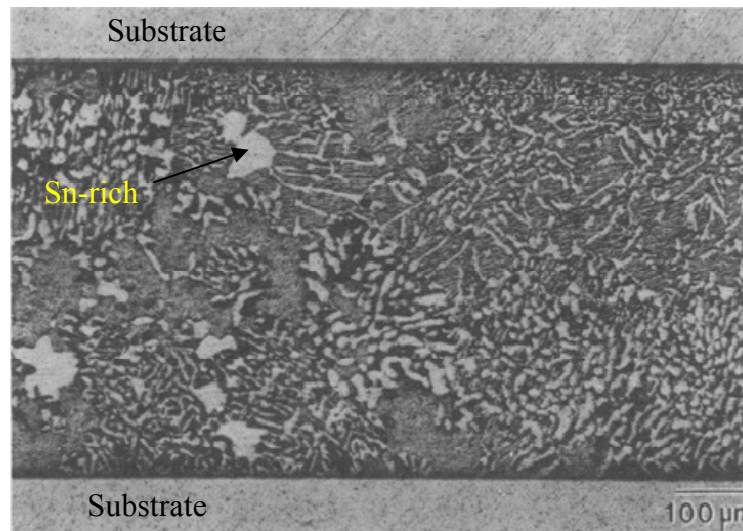


Figure 2.10 Microstructure of eutectic In-Sn solder joint (Goldstein and Morris, 1994)

The microstructure of In-Sn appears to be unaffected by high temperature deformation (Goldstein and Morris, 1994). This is probably due to the extreme softness and ductility of the alloy. Recovery occurs to such a great extent during deformation that the alloy never builds up sufficient driving force to cause interphase boundary migration or nucleation of new grains (Goldstein and Morris, 1994). This lack of coarsening or microstructural rearrangement during high temperature deformation of In-Sn has been confirmed by thermal fatigue studies (Seyyedi, 1993) in which no microstructural changes were observed.

## 2.4.5 Tin-zinc solder alloys

The Sn-9Zn eutectic solder alloy appears to be an attractive alternative, with a melting temperature of 198°C that is relatively close to eutectic tin-lead solder. Phase diagram of Sn-Zn system is shown in Figure 2.11 (Nash and Nash, 1992).

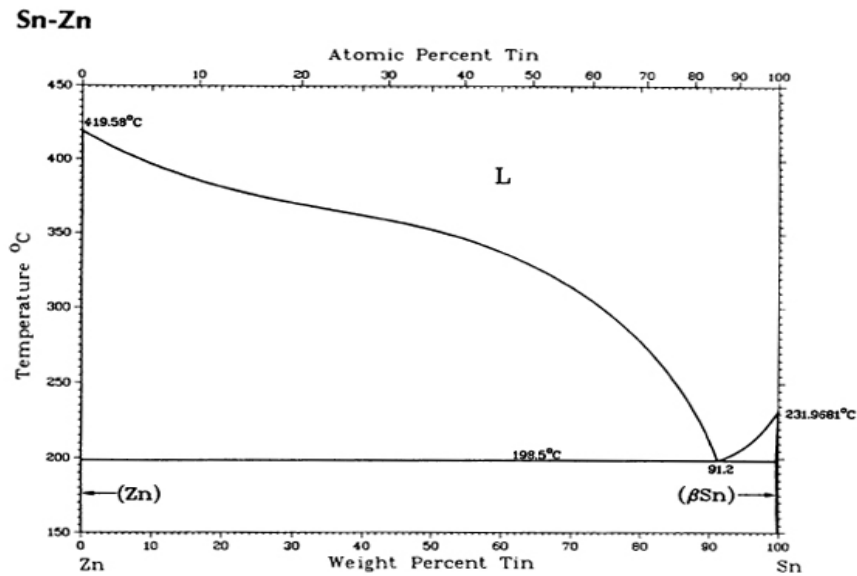


Figure 2.11 Tin-zinc phase diagram (Nash and Nash, 1992)

Tin-zinc eutectic structure consists of two phases: a body centered tetragonal Sn-matrix phase and a secondary phase of hexagonal Zn containing less than 1% tin in solid solution (McCormack *et al.*, 1994). Sn-9Zn is the eutectic composition for the tin-zinc system, and the microstructure can be expected to be lamellar, consisting of alternating Sn-rich and Zn rich phases. Compared to the Sn-Pb system, in the Sn-Zn system, both Sn and Zn interact with Cu to form intermetallic phases, the Cu-Zn compounds are reported to be the primary reaction products. (Suganuma *et al.*, 1998; Chan *et al.*, 2002; Huang *et al.*, 2004). Figure 2.12

shows the Cu-Zn intermetallic formed at the interface of Sn-9Zn/Cu solder joint (Islam *et al.*, 2005).

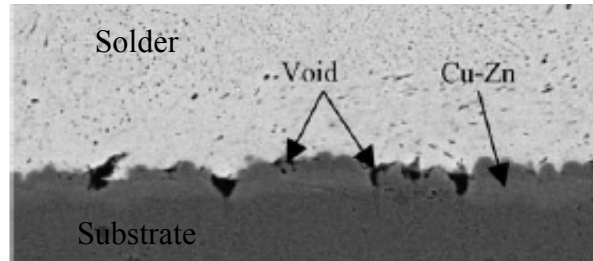


Figure 2.12 Microstructure of Sn-9Zn/Cu solder joint (Islam *et al.*, 2005)

Chen *et al.* (2007) studied the interfacial reactions between eutectic Sn-Zn solder and Cu substrates and reported that the availability of Cu plays an important role in the interfacial reaction between eutectic Sn-Zn solder and Cu. When the Cu substrate is the bulk type, i.e., the supply of Cu is abundant, the  $\text{Cu}_5\text{Zn}_8$  phase is the dominant reaction product. However, when the Cu substrate is the thin-film type, the Zn-rich  $\text{CuZn}_5$  phase becomes the dominant reaction product due to the limited supply of Cu. The  $\text{Cu}_5\text{Zn}_8$  phase in the bulk Cu type remains to be the uniform microstructure after reflow.

## 2.5 Properties of solder alloys

### 2.5.1 Melting temperature

The melting/liquidus temperature is perhaps the first and most important factor of alternative lead-free solder alloys. The melting temperature of eutectic Sn-37Pb solder is  $183^\circ\text{C}$ , and most of the assembly equipment in use is designed to